

Experimental data for high-temperature decomposition of natural celadonite from banded iron formation

K. A. Savko¹ · S. M. Piliugin¹ · N. S. Bazikov¹

Received: 5 March 2015 / Revised: 1 May 2015 / Accepted: 6 July 2015 / Published online: 17 July 2015
© Science Press, Institute of Geochemistry, CAS and Springer-Verlag Berlin Heidelberg 2015

Abstract Three experiments were set up to evaluate conditions for the high-temperature decomposition of celadonite from a banded iron formation in an alumina-free system and identify its decomposition products. It was estimated that at 650 and 750 °C, with a NiNiO buffer and pressure of 3 kbar, celadonite completely decomposes and the decomposition products were tetraferribiotite, magnetite and quartz. Under more oxidizing conditions (hematite-magnetite buffer instead of NiNiO), ferrous potassium feldspar sanidine forms instead of magnetite. During the celadonite decomposition in oxidizing conditions more magnesian and aluminous tetraferribiotite, along with ferrous sanidine, are formed than at reducing conditions.

Keywords Experimental dissolution · Celadonite · Tetraferribiotite · Banded iron formation · Sanidine

1 Introduction

The alkali-enriched banded iron formation (BIF) rocks are common and an important constituent in the Precambrian iron basins. We have identified these BIF as subalkaline type BIF. Rocks of this type are particularly common in the Paleoproterozoic basins of Hamersley, Western Australia (Trendall and Blockley 1970; Miyano and Klein 1983), Transvaal, South Africa (Beukes and Klein 1990) and in the Paleoproterozoic basin of the Kursk magnetic anomaly

(KMA), Russia. Subalkaline BIF contains widespread riebeckite, aegirine, celadonite, tetraferribiotite, and Al-free chlorite instead of grunerite, stilpnomelane, minnesotaite, and greenalite, which are the usual minerals in BIF elsewhere. At the KMA iron deposits, BIF with alkali amphibole were metamorphosed at 370–520 °C and 2–3 kbar (Savko and Poskryakova 2003).

In the KMA, BIF green mica, which is responsible in composition to the celadonite with the formula $\text{KFe}^{3+}(\text{Mg}, \text{Fe}^{2+}) = [\text{Si}_4\text{O}_{10}](\text{OH})_2$, is quite abundant (Savko and Poskryakova 2003). Celadonite forms emerald-green scales sizing from a few tenths to 1.5–2 mm, composing up to 30 %–40 % modal. It intimately intergrows with riebeckite, and the size of their crystals (plates, plaques) in the magnetite layers are larger than those in the quartz layers. The intergrowths of celadonite and riebeckite can form the edges around the coarse grains of carbonate, separating them from the granoblastic quartz aggregate. The riebeckite pseudomorphs occur on celadonite, and very small needles (“seeds”) are found between the riebeckite grains of magnetite and celadonite. Often flakes of celadonite develop on carbonate. The magnetite-celadonite intergrowths form between carbonate and silica matrix. Compositionally, natural celadonite from BIF is extremely low in Al, moderately ferruginous ($X_{\text{Fe}} = 0.27\text{--}0.41$) (Table 1) and is close to ferroceladonite of isomorphic celadonite—ferroceladonite series (Fig. 1).

In addition, BIF celadonite is found in hydrothermally altered mafic volcanic rocks, in sedimentary rocks, especially those with a tuffaceous component under diagenetic or very low-grade metamorphic conditions (Coombs 1954; Wise and Eugster 1964; Boles and Coombs 1975) corresponding to the zeolite facies, and less commonly in the prehnite-pumpellyite and lawsonite-albite-chlorite facies (Landis 1974); however it is not found in the greenschist facies (e.g., Wise and Eugster

✉ N. S. Bazikov
nickolasss@yandex.ru

¹ Voronezh State University, Universitetskaya Square, 1, Voronezh 394088, Russia

Table 1 Chemical composition (wt%) of natural celadonites and synthesized tetraferribioties

	Sample 466-p/131		Obtained under 700 °C, Hem-Mag buffer		Obtained under 650 °C, NiNiO buffer		Obtained under 750 °C, NiNiO buffer	
	Sld-2	Sld-3	Bt-16	Bt-17	Bt-3-650	Bt-6-650	Bt-5-750	Bt-6-750
SiO ₂	50.49	50.85	39.37	39.85	43.61	43.03	39.91	40.00
Al ₂ O ₃	0.49	0.35	0.68	0.59	2.31	2.23	2.10	2.62
TiO ₂	0.01	0.01	0.01	—	0.11	—	0.03	—
FeO	26.15	26.07	33.26	31.51	38.68	39.42	42.13	41.72
MnO	—	—	—	0.19	0.12	0.18	0.18	0.06
MgO	4.80	4.90	14.61	14.37	8.52	7.27	6.52	6.82
CaO	0.05	0.01	0.09	0.40	0.33	—	0.24	0.24
Na ₂ O	0.05	0.04	0.50	0.26	0.17	0.46	0.06	0.26
K ₂ O	10.66	10.35	8.04	9.01	6.03	7.13	8.77	8.20
Total	92.70	92.58	96.56	96.18	99.88	99.72	99.94	99.92
Si	3.77	3.80	3.168	3.272	3.403	3.361	3.192	3.175
Al ^{IV}	0.04	0.03	0.064	0.056	0.212	0.205	0.198	0.245
Fe ³⁺	0.19	0.17	0.768	0.672	0.385	0.434	0.610	0.580
Σ	4.00	4.00	4.00	4.00	4.000	4.000	4.000	4.000
Ti	—	—	0.001	—	0.006	—	0.002	—
Fe ³⁺	1.25	1.19	0.682	0.358	0.079	—	—	—
Fe ²⁺	0.19	0.27	0.564	0.891	2.007	2.141	2.208	2.189
Mn	—	—	—	0.013	0.008	0.012	0.012	0.004
Mg	0.53	0.55	1.753	1.737	0.970	0.847	0.777	0.807
Σ	1.97	2.01	3.00	2.999	3.070	3.000	2.999	3.000
Ca	—	—	0.008	0.034	0.027	—	0.021	0.020
Na	0.01	0.01	0.078	0.041	0.025	0.070	0.009	0.004
K	1.01	0.99	0.825	0.932	0.588	0.711	0.895	0.830
Σ	1.02	1.00	0.911	1.007	0.640	0.781	0.925	0.854
X _{Fe}	0.27	0.33	0.243	0.339	0.696	0.717	0.740	0.731

Sample 466-p/131 Obtained under 700 °C, Hem-Mag buffer Obtained under

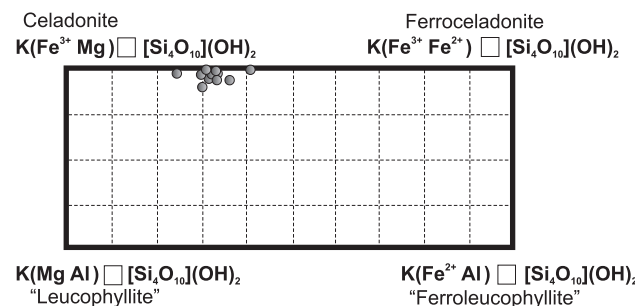


Fig. 1 Compositions of celadonite from KMA BIF shown in a classification plot

1964). Two new minerals of the celadonite family—ferroceladonite and ferroaluminoceladonite—were discovered in the Triassic tuffs (New Zealand) and metamorphosed at the zeolite facies conditions (Li et al. 1997).

Unfortunately, over the past twenty years, no new studies on celadonite behaviour during metamorphism and its thermal stability have appeared. This article is the first

attempt to fill this gap. This topic is very important because currently it is unknown if the minerals, which are the low temperature equivalents of potassium Al-free mica, are unknown as minerals such as glauconite and nontronite contain alumina. In addition, it is not clear what minerals and (or) mineral parageneses are formed by their thermal decomposition due to metamorphism, because potassium pyroxenes, potassium Al-free amphiboles and purely ferruginous K-feldspars are unknown in nature.

The aim of this experimental study is to evaluate conditions for the high-temperature decomposition of celadonite from BIF in an Al-free system and identify its decomposition products.

2 Research procedure

The basis of specimens for the experiments is celadonite monofraction from the borehole 466-R core, sampled at 433 m (Mikhailovsky iron deposit). This ferruginous

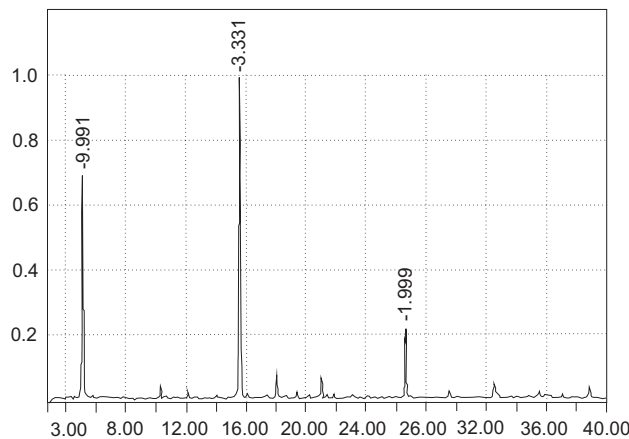


Fig. 2 X-ray diffraction pattern of natural celadonite from KMA BIF. Anode type—Co

quartzite contains 25 % modal celadonite. The sample was pre-crushed in the cast iron pounder, then the obtained powder was sieved on sieves (of diameter 0.316, 0.2, 0.15, 0.1 mm). Then the electromagnetic fraction was extracted from the 0.316 and 0.2 fractions and, finally, 100 mg of celadonite was handpicked under a binomagnifier. Only 40 mg of celadonite was used for the experiments. The composition of natural celadonite is shown in Table 1, the X-ray diffraction pattern in Fig. 2. The mixture was thoroughly mixed and grinded to a powder with an alcohol in the agate pounder. Then it was put into the platinum capsule. The quantity of the initial components calculations were based on the coefficients of the estimated reaction: $\text{Sld} + \text{Qtz} + \text{Mag} = \text{Fe-Kfs} + \text{Gru} (\text{Hyp}) + \text{H}_2\text{O}$, and the molecular weights of Fe, Si, O, K, Mg components. Distilled water was added, and its quantity was consequent to the physical parameters calculations based on the assumed reaction. The platinum capsules were welded and put into gold capsules with a larger diameter. To set the redox conditions, the powder of hematite or NiNiO was used as a buffer, and it was placed between the gold and platinum capsules (Fig. 3). The capsules were weighed, sealed and placed into the rig “high gas pressure apparatus.” Three experiments were conducted: two of them were held with a NiNiO buffer at a pressure of 3 kbar and temperatures of 650 and 750 °C. The values of the temperature and pressure remained constant for 8 days. The third experiment was conducted with a Hem-Mag buffer under the following conditions: T = 700 °C and P = 1 kbar. The data of the temperature and pressure was constant for 4 days. Then the capsules were recovered from installation and were quenched and carefully opened. This material was extracted for further research. Some of this material was investigated with an X-ray diffractometer DRON-4 to clarify the crystal structure of the mineral phases. High-quality experimental powder X-ray

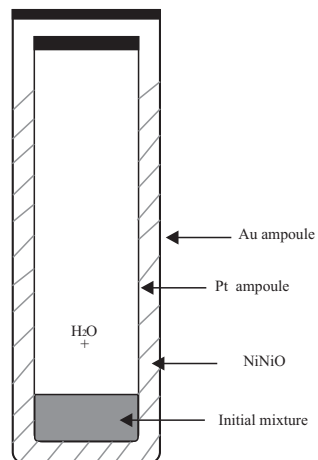


Fig. 3 Scheme of ampoule filling with initial mixture of celadonite and water

diffraction data for the compounds were obtained with an automatic diffractometer DRON-4 (Russia) (fine-focus sealed tube, Co K α 1 radiation ($\lambda = 0.178897$ nm), Johanson's Hybrid Ge{111} monochromator for the primary beam, Bragg–Brentano geometry). The patterns were scanned in reflection mode, $\theta/2\theta$ continuously scanned over the angular range of 3°–40° (2 θ) with a step 0.01° (2 θ) and counting time of 1000 s·step $^{-1}$. Preferred orientation effects were reduced by grinding. Alignment and calibration were checked using Al_2O_3 (SRM676). Diffraction data was collected at room temperature (296 K). The extraction of peak position for indexing was performed with the Pawley method. Unit cell parameters were refined by a least-squares fitting of Bragg's equation to the position of the diffraction lines. All calculations for the refinement of the diffraction patterns and the refinement of the unit cell parameters were performed using the complex programs available in PC software: “HighScore Plus” supplied by PANalytical EMPYREAN [Version: 3.0.t (3.0.5), Date 30-01-2012. Produced by: PANalytical B.V. Amelo, The Netherland]. Another part of this material was used to prepare specimens in order to study the composition and morphology of the mineral individuals in the TESCAN VEGA II XMU electron microscope with an INCA X_SIGHT EDS analyzer at the Institute of Experimental Mineralogy, Russian Academy of Sciences. BSE images and spot analyses of minerals were obtained at a 20 kV accelerating voltage, a beam current of 1.2 mA, counting time of 70 s, and beam 1–3 μm in diameter. The ZAF corrections were introduced during the calculation of oxide concentrations and the installed software of the analytical system assayed the accuracy of the analyses. The accuracy of the analyses was systematically monitored by the replicate analysis of natural and synthetic standards. The cation proportions (crystal-chemical formulae) were calculated by normalizing to four oxygen atoms for magnetite,

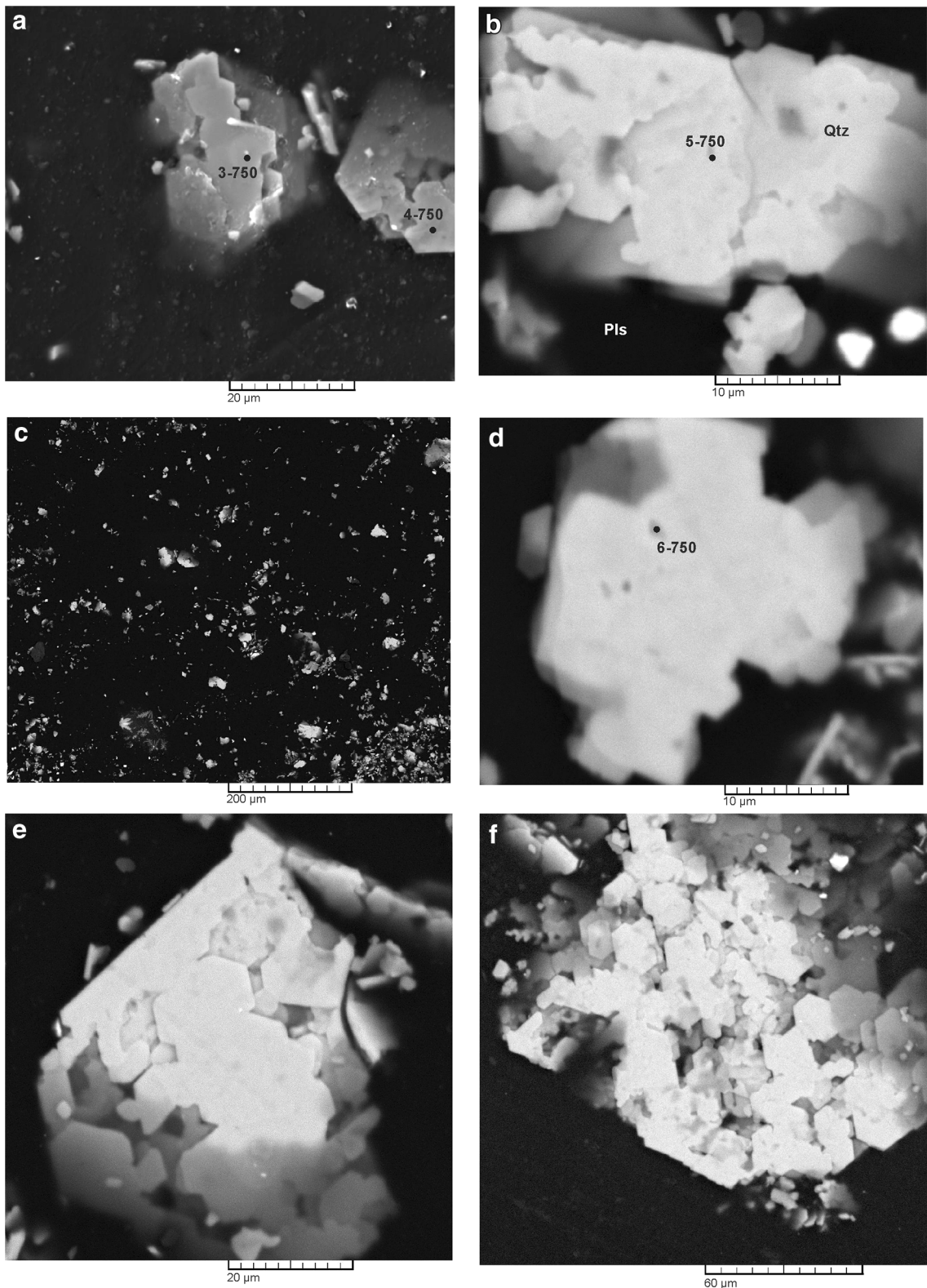


Fig. 4 Mineral individuals obtained during an experiment under 750 °C: **a, b, d**—the obtained mineral; **c**—general view of the sample; **e, f**—mineral forms of tetraferribiotite in the sample. Point numbers correspond the numbers of analyses in Table 1

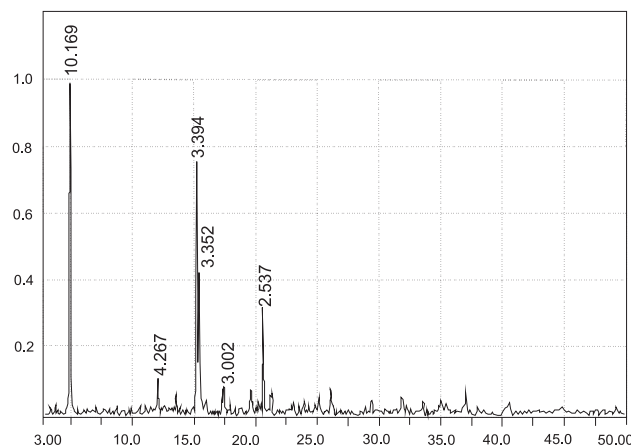


Fig. 5 X-ray diffraction pattern of the sample obtained under 650 °C

eight oxygen atoms for sanidine, and eleven oxygen atoms for tetraferribiotite and celadonite.

3 Experimental results

After experimenting at $T = 650$ and 750 °C (NiNiO buffer), a mixture of tetraferribiotite, quartz and magnetite was obtained, with the quantity of tetraferribiotite dominating over the other phases (Fig. 4). The tetraferribiotite d_{001} values are 10.169 \AA (at 650 °C) and 10.189 \AA (at 750 °C) (see Fig. 5, 6). The natural tetraferribiotite of Hamersley Basin BIF (Western Australia) is characterized by d_{001} 10.159 , 10.163 and 10.180 \AA (Miyano and Miyano 1982). After experimenting at $T = 700$ °C and 1 kbar (Hem-Mag buffer), a mixture of ferrous potassium feldspar, tetraferribiotite, quartz and magnetite was created (Fig. 7).

K-feldspar is made up of small grains of $5\text{--}10\text{ }\mu\text{m}$ (Fig. 7). In composition, this ferruginous potassium feldspar contains Fe_2O_3 from 10.3 to 18.7 wt%, which corresponds to $40.7\text{--}76.6$ mol% minal of ferrous potassium

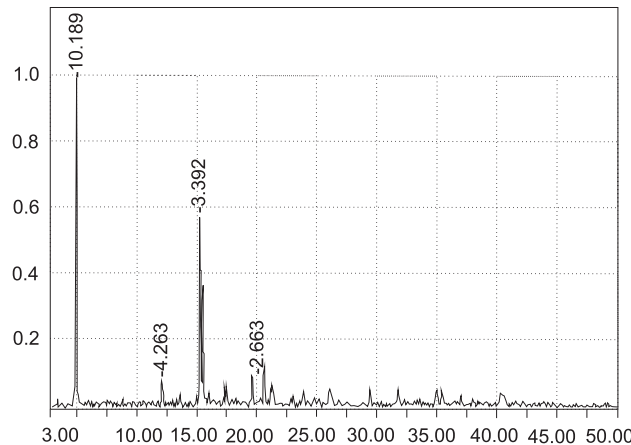


Fig. 6 X-ray diffraction pattern of the sample obtained under 750 °C

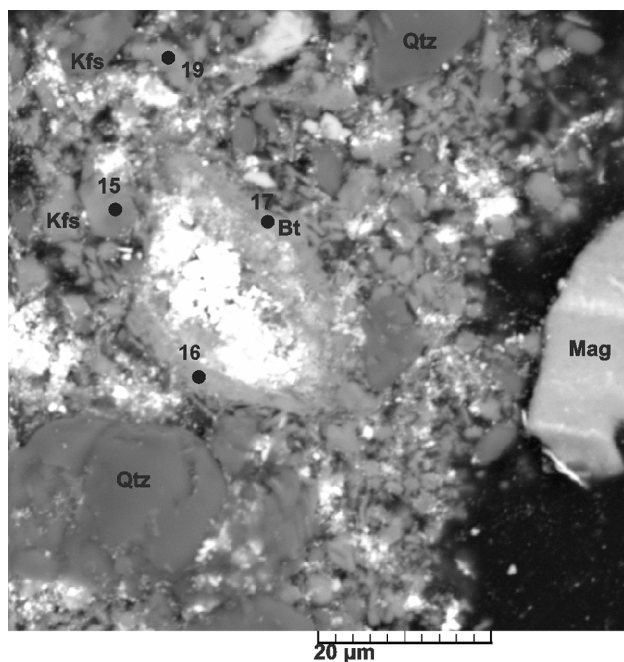


Fig. 7 The obtained mixture of ferrous K-feldspar, tetraferribiotite, quartz and magnetite. Point numbers reflect numbers of analyses in Tables 1 and 2

Table 2 Chemical composition (wt%) of synthesized ferrous sanidines

	Kfs-1	Kfs-2	Kfs-3	Kfs-4	Kfs-5
SiO_2	63.24	63.99	63.79	60.89	62.62
Al_2O_3	6.4	5.47	9.61	3.65	6.21
TiO_2	0.13	0.02	—	—	—
FeO	14.68	14.91	10.33	18.68	15.71
MnO	0.05	0.01	—	0.06	0.09
MgO	0.35	0.59	0.31	1.56	0.85
CaO	0.85	0.97	0.22	1.67	0.17
Na_2O	0.01	0.23	0.18	0.49	0.14
K_2O	14.30	13.74	15.51	12.93	14.09
Total	100.01	99.99	100.00	99.94	99.97
Si	3.063	3.093	3.055	3.003	3.042
Al^{IV}	0.365	0.312	0.542	0.212	0.355
Fe_{3+}	0.535	0.542	0.372	0.693	0.574
Σ	3.963	3.947	3.969	3.908	3.971
Ca	0.044	0.050	0.011	0.088	0.009
Na	0.001	0.022	0.017	0.047	0.013
K	0.884	0.847	0.948	0.814	0.873
Σ	0.929	0.919	0.976	0.949	0.894
Ort	0.952	0.922	0.971	0.858	0.976
Ab	0.001	0.024	0.018	0.049	0.014
An	0.047	0.054	0.011	0.093	0.010
Fe-Fsp	0.594	0.635	0.407	0.766	0.618

feldspar (Table 2) with 3.65 to 9.61 wt% Al_2O_3 . The quantities of albite and anorthite components are 0.1–4.9 and 1.0–5.3 mol%, respectively.

X-ray diffraction study of K-feldspar (Fig. 7) has shown that K-feldspar is made up of ferrous sanidine, for which the resulting diffraction pattern on the lattice parameters were calculated using UnitCell (Holland and Redfern 1997a, b): $a_0 = 8.634(5)$, $b_0 = 13.276(5)$, $c_0 = 7.194(5)$ Å, $\beta = 116.79(2)^\circ$, $V = 736.2$ Å 3 . These values are close to the unit lattice parameters for the refined structure, synthesized low sanidine which has the following composition: $\text{K}_{0.93}(\text{Al}_{0.75}\text{Fe}_{0.27})\text{Si}_{3.01}\text{O}_8$ (Nadezhina et al. 1993): $a_0 = 8.627$, $b_0 = 13.058$, $c_0 = 7.209$ Å, $\beta = 116.00^\circ$, $V = 730.0$ Å 3 .

Tetraferribiotite synthesized with Fe-sanidine appears in the shape of elongated 15–20 microns flakes (Fig. 7). On the diffraction pattern it is defined by a clear characteristic reflex of 10.234 Å (Fig. 8). The tetraferribiotite obtained in the experiment is characterized by low-Al ($\text{Al}_2\text{O}_3 = 0.59$ –0.68 wt%) and iron (0.243–0.339 at. u.), due to the significant prevalence of Fe^{3+} over Fe^{2+} in the structure (Table 1). Tetraferribiotite synthesized at more reducing conditions (buffer NiNiO) has significantly more iron (0.696–0.740 at. u.) and alumina ($\text{Al}_2\text{O}_3 = 2.10$ –2.62 wt%) (Table 1). In composition, tetraferribiotites synthesized under more oxidizing conditions (Hem-Mag buffer) are closer to the natural tetraferribiotites in the KMA BIF (Savko and Poskryakova 2003), with higher concentrations of Fe^{3+} and Mg and lower Fe^{2+} , and approaching tetraferriphlogopite (Fig. 7).

4 Discussion

Tetraferribiotite, a fairly rare Al-free mica, with a formula of $\text{K}(\text{Mg},\text{Fe}^{2+},\text{Fe}^{3+})_3[\text{Fe}^{3+}\text{Si}_3\text{O}_{10}] (\text{OH})_2$, was first discovered in 1955 during an unsuccessful experimental effort

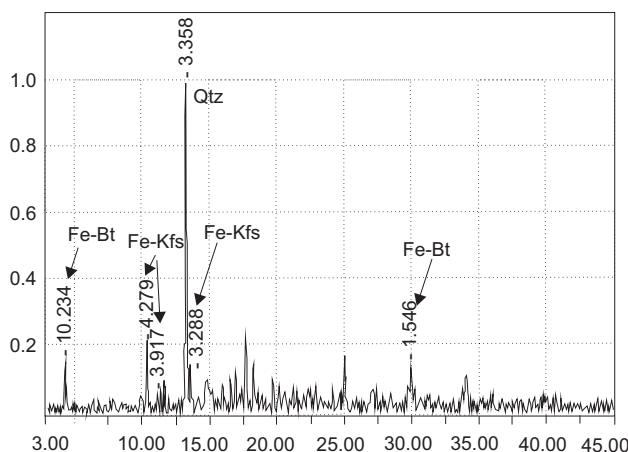


Fig. 8 X-ray diffraction pattern of synthesized ferrous sanidine, tetraferribiotite and quartz

to synthesize K-OH amphibole (Veres et al. 1955). One member of the tetraferribiotite group, ferriannite, was synthesized in the experiments of D.R. Wones (1963) within the temperature range of 400–850 °C, pressure range of 1035–2070 bar, and an oxygen fugacity between the hematite–magnetite and iron–wuestite buffers. He has suggested that mica of ferriannite composition should occur in magmatic Fe-rich rocks. But later ferriannite was described in the riebeckite-bearing rocks in the BIF of Western Australia (Miyano and Miyano 1982) and South Africa (Miyano and Beukes 1997).

Tetraferribiotite occurs in the iron formation of the Mikhailovskoe mining district as small reddish-brown flakes, 0.2–1.0 mm across, in association with magnetite, hematite, riebeckite, aegirine, celadonite, and carbonate. Compared with celadonite, the mineral occurs in subordinate amounts. It is preferably localized in magnetite-hematite layers as disseminated flakes, although it can occasionally also be composed of nearly monomineralic thin layers with merely minor amounts of celadonite and iron oxides. Tetraferribiotite sometimes forms inclusions in aegirine, although these rocks may not contain this mineral in the groundmass.

Tetraferribiotite in the KMA BIF is less aluminous ($\text{Al}_2\text{O}_3 = 0.68$ –0.76 wt%) and more magnesian ($\text{MgO} = 10.13$ –14.09 wt%) than natural ferriannite (Miyano and Miyano 1982; Miyano and Beukes 1997), whose Al_2O_3 content is always higher than 1.3 wt%, usually about 4–5 wt%, and whose MgO concentration varies from 3.5 to 12.5 wt% (Fig. 9). The Si/Al ratio of the tetraferribiotite is always one order of magnitude higher than 3.0. Thus, the compositions of the KMA BIF tetraferribiotite are closest to those of the end member of the annite-ferriannite series, and shift toward tetraferriphlogopite in the tetraferriannite-tetraferriphlogopite series (Fig. 9).

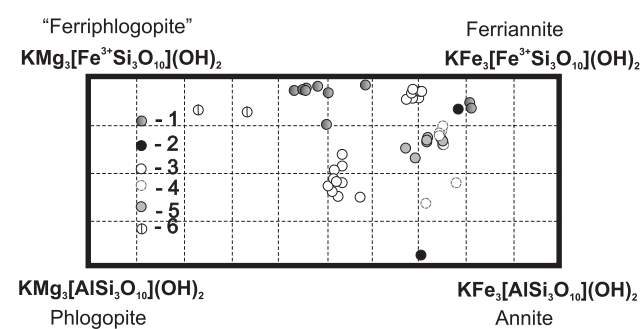
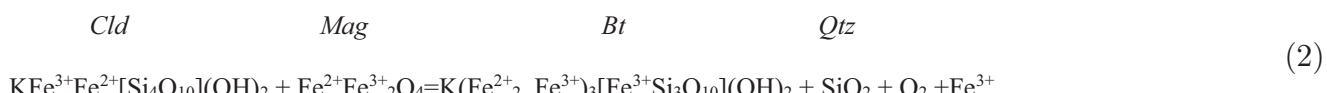
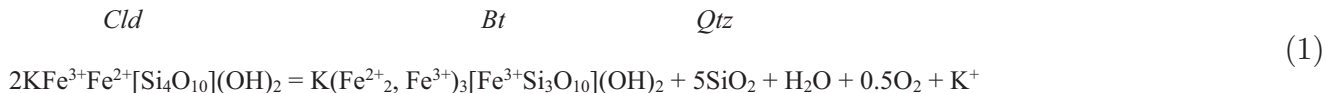


Fig. 9 Compositions of tetraferribiotites shown in a classification plot. 1—KMA BIF (Savko and Poskryakova 2003); 2—Penge iron formation, South Africa (Miyano and Beukes 1997); 3—Dales George iron formation, Western Australia (Miyano and Miyano 1982); 4—synthesized under 650 °C (NiNiO buffer); 5—synthesized under 750 °C (NiNiO buffer); 6—synthesized under 700 °C (Hem-Mag buffer)

The results of the experiments carried out at 650–750 °C and under different redox conditions (NiNiO and Hem-Mag buffers) suggest that, at smaller values of $f\text{O}_2$ (buffer NiNiO), tetraferribiotite and quartz are formed by celadonite decomposition. With higher values (Hem-Mag buffer) the breakdown products are tetraferribiotite, ferrous sanidine and quartz. The celadonite breakdown reactions in the system $\text{SiO}_2-\text{Fe}_2\text{O}_3-\text{FeO}-\text{K}_2\text{O}-\text{O}-\text{H}$ for different $f\text{O}_2$ —(1) and (2) for NiNiO buffer and (3) to Hem-Mag buffer are shown below.



The celadonite breakdown reaction (3) to form ferrous potassium feldspar and tetraferribiotite is illustrated on the diagram ($\text{Mg} + \text{Fe}^{2+}$)– Si –($\text{Al} + \text{Fe}^{3+}$) (Fig. 10).

It is important to point out that, at more oxidizing conditions (Hem-Mag buffer) with Fe-sanidine, more Mg and Al enriched tetraferribiotite is formed than at reducing conditions (NiNiO buffer). In addition, during celadonite decomposition (NiNiO buffer) ferrous feldspar was not obtained. Differences in the iron content in tetraferribiotite were due to the fact that, under more oxidizing conditions, the ratio of $\text{Fe}^{3+}/\text{Fe}^{2+}$ increased

and $\text{Fe}^{2+}/(\text{Fe}^{2+}+\text{Mg})$ decreased accordingly. Lower alumina content in tetraferribiotite synthesized on the Mag-Hem buffer is due to the simultaneous formation of ferrous sanidine, which contains from 3.6 to 9.6 wt% Al_2O_3 (Table 2). Thus, a small amount of the alumina from decomposed celadonite became included in the structure of the formed ferrous sanidine.

Similar results were found earlier for the thermal decomposition of synthetic celadonite under different redox conditions (buffers QFM, NiNiO, Mag-Hem) (Wise

and Eugster 1964) at pressures of 1–3 kbar. However, as noted by the authors, the experimentally determined upper limit of celadonite stability is about 410 °C and doesn't correspond to the breakdown temperature of celadonite in natural systems. Moreover, they believed that, in nature, celadonite decomposes at temperatures below 400 °C on the boundary of the zeolite and greenschist facies.

The evaluation of metamorphic conditions for the Paleoproterozoic KMA BIF show that celadonite in the ferruginous quartzites was stable during metamorphism above 520 °C at a pressure of 3 kbar (Savko and Poskryakova 2003).

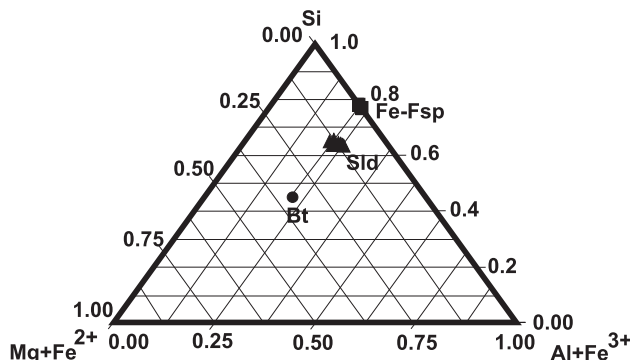


Fig. 10 Celadonite breakdown with ferrous K-feldspar and tetraferribiotite formation shown in the ($\text{Mg} + \text{Fe}^{2+}$)– Si –($\text{Al} + \text{Fe}^{3+}$) diagram

5 Conclusion

As a result of conducting an experiment at 700 °C and 1 kbar with a Hem-Mag buffer, natural dioctahedral mica Al-free celadonite was completely decomposed to form ferrous sanidine ($\text{Fe-Fsp} = 0.407\text{--}0.766$ at. u.) and trioctahedral Al-free mica (tetraferribiotite). In the experiments at 650 and 750 °C and 3 kbar, with a NiNiO buffer, the complete decomposition of celadonite gave tetraferribiotite, magnetite and quartz. Thus, according to the results of our experiments, we can draw the following conclusions:

- (1) Ferrous sanidine, tetraferribiotite and quartz are formed during the thermal dissolution of celadonite at relatively high values of $f\text{O}_2$ —on hematite-magnetite buffer. At more reduced conditions (buffer NiNiO), potassium feldspar is not formed and the breakdown products are tetraferribiotite, magnetite and quartz.
- (2) During celadonite decomposition in more oxidizing conditions (Hem-Mag buffer) with Fe-sanidine, more Mg and Al enriched tetraferribiotite is formed than at reducing conditions (NiNiO buffer).

References

- Beukes N, Klein C (1990) Geochemistry and sedimentology of a facies transition from microbanded to granular iron-formation in the early proterozoic transvaal supergroup, South Africa. *Precambrian Res* 47:99–139. doi:10.1016/j.precamres.2011.03.031
- Boles JR, Coombs DS (1975) Mineral reactions in zeolithic Triassic tuff, Hokonui Hills, New Zealand. *Geol Soc Am Bull* 86: 163–173
- Coombs DS (1954) The nature and alteration of some Triassic sediments from Southland, New Zealand. *Trans R Soc N Z* 82:65–109
- Holland TJB, Redfern SAT (1997a) Unit cell refinement from powder diffraction data: the use of regression diagnostics. *Miner Mag* 61:65–77
- Holland TJB, Redfern SAT (1997b) UNITCELL: a nonlinear least-squares program for cell-parameter refinement implementing regression and deletion diagnostics. *J Appl Cryst* 30:84
- Landis CA (1974) Stratigraphy, lithology, structure, and metamorphism of Permian, Triassic, and Tertiary rocks between the Mararoa River and Mount Snowdon, western Southland, New Zealand. *J R Soc N Z* 4:229–251
- Li G, Peacor DR, Coombs DS, Kawachi Y (1997) Solid solution in the celadonite family: the new minerals ferroceladonite, $\text{K}_2\text{Fe}_2^{2+}\text{Fe}_2^{3+}\text{Si}_8\text{O}_{20}(\text{OH})_4$, and ferroaluminoceladonite, $\text{K}_2\text{Fe}_2^{2+}\text{Al}_2\text{Si}_8\text{O}_{20}(\text{OH})_4$. *Am Mineral* 82:503–511
- Miyano T, Beukes NJ (1997) Mineralogy and petrology of the contact metamorphosed amphibole asbestos-bearing Penge iron formation, Eastern Transvaal, South Africa. *J Petrol* 38:651–676
- Miyano T, Klein C (1983) Conditions of riebeckite formation in the iron formation of the Dales Gorge Member, Hamersley Group, Western Australia. *Am Mineral* 68:517–529
- Miyano T, Miyano S (1982) Ferri-annite from the Dales George Member iron-formations, Wittenoom area, Western Australia. *Am Mineral* 67:1179–1194
- Nadezhina TN, Pushcharovskiy DY, Taroev VK, Tauson VI, Bychkov AM (1993) Crystal structure of ferrialuminosilicate low sanidine. *Kristallografiya* 38(6):77–82 (in Russian)
- Savko KA, Poskryakova MV (2003) Riebeckite–aegirine–celadonite BIF at the Mikhailovskoe Iron Deposit of the Kursk Magnetic Anomaly: phase equilibria and metamorphic conditions. *Petrology* 11(5):426–443
- Trendall AF, Blockley JG (1970) The iron formation of the Precambrian Hamersley Group, Western Australia with special reference to the associated crocidolite. Western Australia, Geological Survey of Western Australia
- Veres GI, Merenkov TB, Ostrovsky IA (1955) Artificial pure ferrous hydroxyl mica. *Dokl Akad Nauk SSSR* 101(1):147–150 (in Russian)
- Wise WS, Eugster HP (1964) Celadonite: synthesis, thermal stability and occurrence. *Am Mineral* 49:1031–1083
- Wones DR (1963) Phase equilibria of “ferriannite”, $\text{KFe}_3^{+2}\text{Fe}^{+3}\text{Si}_3\text{O}_{10}(\text{OH})_2$. *Am J Sci* 261:581–596